UCLA
UCLA Electronic Theses and Dissertations

Title

Microparticle Production Using 3D-Printed Microfluidic Devices

Permalink

https://escholarship.org/uc/item/3nv6k71h

Author

Aburime, Leon

Publication Date

2024

Supplemental Material

https://escholarship.org/uc/item/3nv6k71h#supplemental

Peer reviewed|Thesis/dissertation

UNIVERSITY OF CALIFORNIA

Los Angeles

Microparticle Production Using 3D-Printed Microfluidic Devices

A thesis submitted in partial satisfaction

of the requirements for the degree Master of Science in Bioengineering

by

Leon Aburime

2024

ABSTRACT OF THE THESIS

Microparticle Production Using 3D-Printed Microfluidic Devices

by

Leon Aburime

Master of Science in Bioengineering

University of California, Los Angeles, 2024

Professor Dino Di Carlo, Chair

Microfluidic applications often face challenges such as costly cleanrooms, single-level designs, and labor-intensive preparation processes prone to errors. These constraints hinder laboratories needing cost-effective methods for microfluidic research. Fortunately, 3D printing technology, with its improving resolution, offers a promising solution. 3D printing allows for a less laborious, more scalable approach to creating complex, multi-level microfluidic devices. However, developing an effective droplet generator involves challenges like precise droplet size control, uniform production, and managing fluid dynamics. This thesis addresses these issues by introducing a novel method for producing drug-laden microparticles using a high-throughput, branched, multi-level droplet generator, all implemented with a commercially available 3D printer and free CAD and slicer software. This advancement enables researchers to share and create innovative designs swiftly, reducing both time and cost.

The thesis of Leon Aburime is approved.

Song Li

Jacob J. Schmidt

Dino Di Carlo, Committee Chair

University of California, Los Angeles

2024

CONTENTS

1.   **Introduction**:
1.1 Background of microfluidic devices
1.2 The importance and advantages of 3D printing in this field
1.3 Research question or hypothesis

2.   **Literature Review**:
2.1 An overview of current methods for creating microfluidic devices
2.2 Limitations of current methods
2.3 Introduction to 3D printing techniques and their applications in microfluidics

3.   **Materials and Methods:**
3.1 Details of the 3D printers used
3.2 Information on the resins and photoabsorbers
3.3 Description of the printing process.
3.4 Precursor composition of microparticles
3.5 Microparticle Fabrication

4.   **Results:**
4.1 Presentation of gathered data, including images, measurements, & other relevant results
4.2 Implications of findings in the broader context of microfluidics and 3D printing

5.   **Discussion**:
5.1 Interpretation of results
5.2 Challenges faced and potential solutions

6.   **Conclusion**:
6.1 Summary of the main findings
6.2 Potential applications of research
6.3 Recommendations for future research

7.   **Recommendations**: Specific steps or strategies that can be taken based on findings.

8.   **References**: A list of all the sources you referenced throughout thesis.

9.   **Appendix**: Any supplementary information, raw data, or additional details that support research but aren't essential for the main body.

List of Figures

ACKNOWLEDGMENTS

I would like to thank Vivek Rajasenan who taught me everything about 3D SLA printing. He guided me in the early days when I knew nothing and it would have been impossibly long, hard, and time-consuming to learn by myself as well as to iterate or problem-solve when I got stuck.

I would like to thank my lab mates and friends who were always there to help whenever I had questions or needed something. I also want to thank ChatGPT for helping me write in prose that leads to a level of clarity and professionalism that would have been difficult to achieve on my own.

Thank you to my P.I. Dino Di Carlo for allowing me to pursue intellectually appealing experiments, acting as a mentor, and supporting me throughout my time at UCLA.

Introduction:

1.1 Background of microfluidic devices

Microfluidic devices, often called "labs-on-a-chip", are devices that can be used for a range of applications as they allow for precise control and manipulation of fluids at the microscale. They generally consist of microchannels, chambers, and valves in substrates like silicon, glass, or polymers. Their design capitalizes on the unique fluid dynamics that emerge at the microscale, where laminar flow and surface, inertial, frictional and viscous forces dominate over gravitational forces and are harder to predict or control(Xue et. al 2011). As a result, microfluidics allows for higher precision in desired fluid behavior to be exploited for various sectors in chemistry, biology, and engineering.

Droplet microfluidics are a popular method of generating microparticles that can be used in a range of applications such as drug delivery, diagnostics, cell capturing and profiling, contained chemical reactions and more . Unfortunately, using photolithography to produce microfluidic devices is a time and resource-intensive process that often needs expensive microfabrication facilities. Currently, polydimethylsiloxane(PDMS) is a popular choice due to its biocompatibility, transparency, and relatively low cost. However, PDMS is a hydrophobic gel that needs time to harden and cannot typically be used to create multiple levels, where different design architectures can be stacked vertically

Such a wide range of use cases can be seen in projects where devices are used to rapidly sequence DNA, allow for point-of-care diagnostics, and even in single-cell dynamics and tissue engineering(Jayamohan et. al 2013). Beyond biomedicine, microfluidics can be seen in high-throughput screening, droplet-based reactions, and syntheses that benefit from rapid heat

and mass transfer. Environmental applications include on-site monitoring of pollutants and pathogens, while in pharmacology, they offer platforms for drug discovery and pharmacokinetics(Damiati 2018). This versatility stems from the adaptability of microfluidic systems that can be used to address specific challenges that are hard to work with due to the size of materials involved, such as cells, molecules, polymers, and more.

1.2 The importance and advantages of 3D printing in this field

The emerging discipline of microfluidics has witnessed significant advancements with the incorporation of 3D printing technology. The advantage of 3D printing in this field comes from its ability to rapidly prototype and produce intricate and custom microfluidic designs such as those with curved, unique or non-traditional shapes, vertical structures, and profiles that are hard to fabricate on a photoresist or would otherwise be challenging, time-consuming and unreasonably costly. This capability enables researchers and developers to iterate and refine their blueprints using Computer-Aided Design(CAD), thereby accelerating the pace of innovation in microfluidic applications.

Additionally, 3D printing offers many advantages such as design flexibility and geometric freedom. It allows for the creation of complex internal structures, including architectures and multi-layered channels, that are often difficult to achieve with standard soft lithography methods that use PDMS. This versatility broadens the number of potential applications and permits widespread use, especially in drug delivery by allowing drug-laden microparticles to degrade over long periods and therefore save patients medication costs, doctor visits, repeated painful injections, side effects from high dosages, and more. This would allow researchers who do not

have access to a clean room or lack employees or student researchers to craft sophisticated microfluidic devices at a fraction of the cost and time with these CNC machines.

1.3 Research question or hypothesis

An important question is raised regarding the creation of modern microfluidic devices: Can the automated nature of SLA 3D printing be the key to overcoming current device fabrication challenges? SLA's ease in layering and its ability to handle complexity could be critical, especially when faced with the difficulties of layered designs and the use of materials like PDMS.

Building on this, there's a hypothesis to consider: Could SLA 3D printing be the answer to creating multi-layered microfluidic devices for biomedical uses? By harnessing SLA, is it possible to make devices that create small droplets- under 200 um - from multiple parallel channels to drastically increase droplet throughput that can be used for long-term drug delivery? Success could mean not just a new, simpler way to make devices, but also a big leap in how to scalably produce drug-loaded microparticles.

Literature Review:

2.1 An overview of current methods for creating microfluidic devices

Generally, to create microfluidic chips, a master template is fabricated in a clean room where patterns are transferred from a mask to a photosensitive material or photoresist on a substrate. Once exposed to ultraviolet light through the mask, the exposed or unexposed regions (based

on the photoresist) can be washed away, leaving behind the desired microscale structures that are used to define the micro or nano-sized channels. Then the etching process is used to actually carve out microchannels where the length of time controls the height of the channels. (Scott 2021)
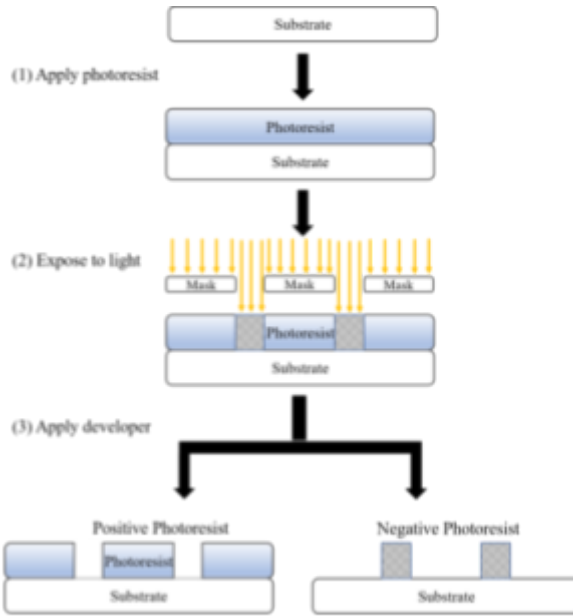
Once the photoresist mold has been created polydimethylsiloxane (PDMS), a transparent and biocompatible elastomer, is mixed with a curing agent and poured over the prepared master mold. The mixture is then cured at higher temperatures to transform it from a liquid state to a flexible solid. After the PDMS is cured it's peeled off the master mold, revealing negative microstructures and channels that are exact replicas of the master mold's design. After the PDMS is removed it is bonded, usually via oxygen plasma treatment to increase adhesion, to another surface such as another PDMS layer, glass, or other substrates. This process typically involves a cleanroom, etching processes, substrate treatments, and additional polymers such as PDMS which can only be used as a template to create one-layer devices. (Lin et. al 2021)

Figure 1. The photoresist process

2.2 Limitations of current methods.

While microfluidics has come a long way it is still plagued by many problems. The lithography process to create the master molds is time and resource-intensive, which slows down rapid prototyping. When minor changes need to be made, a new stamp must be fabricated even if the new iteration may not work. The costs associated with establishing and maintaining a cleanroom to even create these molds further strain scalability. (Walsh et. al 2017)

2.3 Introduction to 3D printing techniques and their applications in microfluidics

In the realm of 3D printing, various technologies have emerged to address the requirements of microfluidic device fabrication. One such notable technique that offers much-needed precision is the LCD-based 3D printer. This approach utilizes the properties of light manipulation and liquid crystal technology to create detailed structures from CAD designs.

How does a 3D LCD Stereolithography printer work?

An LCD 3D printer operates using a complex assembly of components that work together to transform digital designs into physical objects. The core of this printer is a series of high-powered light-emitting diodes (LEDs), which are the primary source of light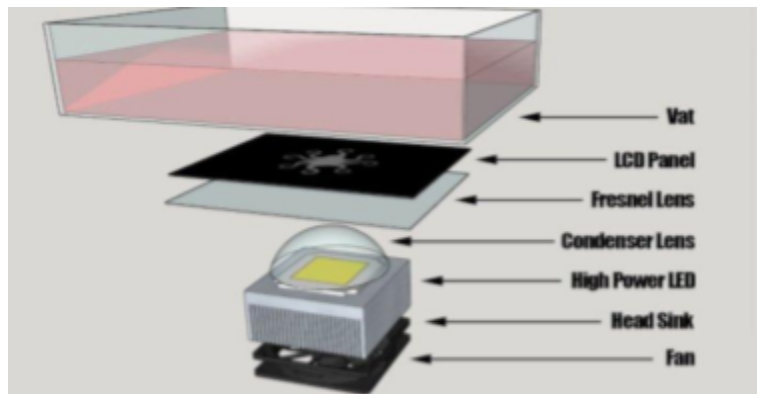 for curing the resin. These LEDs are arranged in such a way that their light is first passed through a convex lens. This lens acts to condense the light from the LEDs into a single, more intense light

Figure 2: Configuration of a SLA 3D Printer

source. The condensed light is then directed through a Fresnel lens, which further focuses the light into a narrower, more precise beam. This concentrated beam of light is essential for the accuracy and resolution of the printing process, as it ensures that the light is precisely directed where it is needed.

The focal point of this light system is the liquid crystal display (LCD) situated beneath the resin vat. The LCD plays a critical role in the printing process: it displays the specific pattern of each layer of the design that the user intends to create. The photopolymerizable resin, which fills the vat above the LCD, is sensitive to the specific wavelength of light emitted by the LEDs. As the focused light passes through the displayed pattern on the LCD, it cures the resin in the exact shape of that pattern. Layer by layer, the LCD updates to reflect the next cross-section of the design, and the printer cures the resin accordingly, building the 3D object from the bottom up. This process of using light to solidify resin in a layer-by-layer fashion is what enables LCD 3D printers to produce highly detailed and complex structures with a high degree of precision.

Materials and Methods:

3.1 Details of the 3D printers used.

The 3D printer employed for this research is the Phrozen Sonic Mini 8K Resin 3D Printer, ordered from Amazon. This 8K is known for its high resolution and precision, crucial for the fabrication of microfluidic devices. The Sonic Mini 8K operates using the Stereolithography (SLA) 3D printing technology, which is particularly suitable for creating intricate multi-level microfluidic devices aimed in this study.

3.2 Information on the resins and photoabsorbers.

In the development of 3D-printed microfluidic chips, the selection and preparation of resins and photoabsorbers are crucial to achieving desired properties in the final device. For this project, Blu Resin by Siraya Tech, a clear and viscous hydrophobic resin, is employed as the primary printing material. Blu Resin is known for its high strength and durability, making it an excellent choice for microfluidic applications where structural integrity and longevity are essential. It's clear makeup also facilitates visual access inside the channels of the microfluidic device, a critical feature that helped ensure channels were indeed printing at smaller scales. The hydrophobic characteristic of Blu Resin aligns well with microfluidic applications where the control of fluid flow is paramount, particularly in droplet generation. In these applications, it is crucial that the resin prevents the wetting of channel surfaces to ensure that droplets form correctly and do not spread out along the channels. Proper wetting properties are essential to maintain the integrity of the droplet formation process, allowing droplets to be sheared off cleanly rather than adhering to the channel walls. This characteristic is particularly important for the prevention of hydrophilic wetting of future microparticles, ensuring that they maintain their intended shape and size during and after formation.

To adjust the resin's properties for specific light-curing capabilities, Sudan 1, a red hydrophobic photoabsorber, is mixed with Blu Resin. Sudan 1 is known for its ability to absorb specific wavelengths of light, which is needed to control the resin's curing process during 3D printing at a wavelength of 405 nm. This photoabsorber is mixed thoroughly with the Blu Resin, a process that can take several hours to days due to its high viscosity, depending on the concentration of

Sudan 1 used. The mixing is done using a magnetic plate and pill stirrer, ensuring a homogeneous distribution of Sudan 1 within the resin. The duration of mixing, sometimes for several days with 0.2% Sudan 1, is a critical parameter as it directly influences the even dispersion of the photoabsorber throughout the resin, thus affecting the uniformity of curing during the printing process.

3.3 Description of the printing process.

The process of fabricating the microfluidic devices using 3D printing technology begins with a meticulous design phase. Initially, the chip is designed in Autodesk Fusion 360, a versatile CAD software that allows for precise modeling of the microfluidic channels and structures. Once the design is finalized, it is exported as an STL file, a common file format compatible with most 3D printers. This file format represents the surface geometry, or series of connected triangles, of the modeled device, which is essential for accurate 3D printing.

The next step involves importing the STL file into Chitubox, a slicing software specifically for resin 3D printing. Chitubox translates the 3D model into a series of layers and generates the corresponding G-code, which is a programming language that instructs the 3D printer. In Chitubox, certain print settings are adjusted, such as layer height, exposure time, and bottom exposure time. These settings are important, as they dictate the curing time of each layer of resin, influencing the resolution and stability of the printed structures. Notably, when the exposure time is too long the resins can clog the internal channels but if they are too short the channels may not maintain their shape as they rupture too easily, especially during initial cleaning. After the setup in Chitubox is complete, the file is sent to the 3D printer.

When developing 3D-printed microfluidic devices for droplet generation, several significant challenges needed to be addressed to achieve reliable performance. One major hurdle was optimizing the surface chemistry of the channels to ensure proper droplet formation. The hydrophobic properties of the Sudan 1-mixed Blu resin were crucial to prevent the wetting of channel surfaces and ensure that droplets formed correctly without spreading along the internal walls. This required careful selection and testing of different resin formulations with varying viscosity profiles manufactured by Sirayatech to balance hydrophobicity with other material properties like post-UV-cured polymer strength needed for device stability and function.

Another critical challenge was controlling the dimensions of the microfluidic channels. Precise channel dimensions are essential for maintaining consistent fluid flow and droplet size. Inaccurate dimensions can lead to uneven pressure distribution and inconsistent droplet formation. Additionally, the polymerization process itself posed difficulties; ensuring that all channels were fully cured without leaving any unpolymerized resin was vital to prevent clogging and device failure. Clearing unpolymerized resin from the channels often required post-processing, which included multiple cleaning steps with solvents like ethanol to ensure the channels were free of any residual resin.

In an attempt to replicate a 200-channel microfluidic device described in the 2019 paper by de Rutte et al., which featured separate inlets for the dispersed and continuous phases
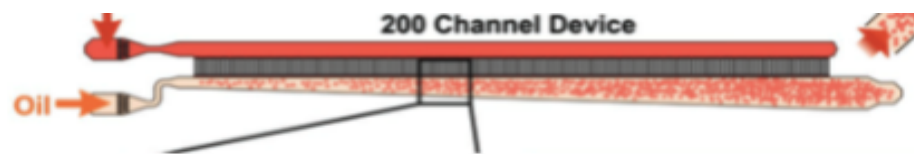

Figure 3: Parallelized High-Throughput Schematic from de Rutte(2019)

(as illustrated in Figure 3), challenges were encountered when utilizing the Sudan 1-mixed

hydrophobic resin. The original device's design, with all channels aligned in parallel, presented a significant obstacle when adapted to the properties of the hydrophobic resin. The primary issue arose from the pressure differences across the device, from the inlet to the terminal channels. While the channels near the inlet were able to form droplets effectively, those towards the end of the device encountered difficulties. The dispersed phase liquid failed to reach these final channels without the application of exceedingly high pressures- pressure that, if maintained, resulted in device rupture. This limitation resulted in a new design that tried to redistribute the pressure evenly from the start using a branched design.(de Rutte et. al 2019)

Shear-Free Microfluidic Droplet Generator

A shear-free device is a microfluidic chip that doesn't require shear force from the continuous phase to 'shear' the dispersed phase off to produce small droplets. Shear-free configurations are preferred because they are easier to clean as the fluid only flows one way, only requiring tubing at one inlet and no outlets while a shear-thinning device requires tubing for two inlets and one outlet thus adding to the time and material it takes to make it operational. For the current shear-free device, a branched bifurcated design(Figure 4)
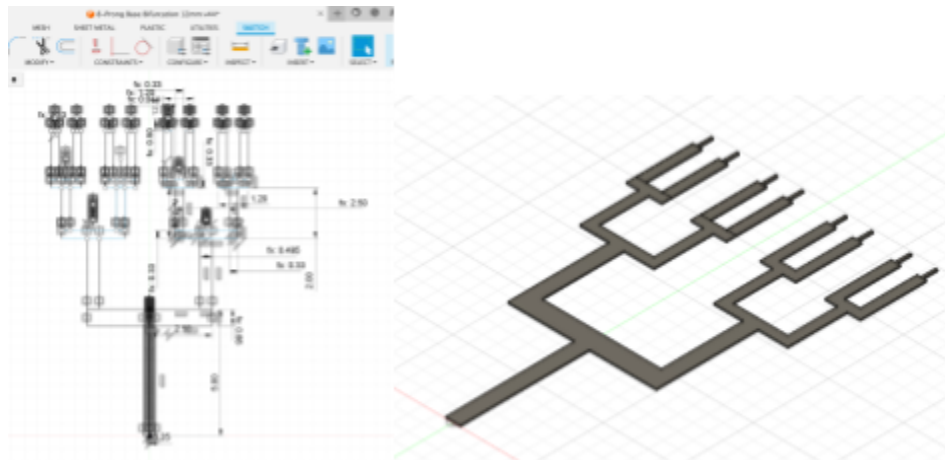

Figure 4: CAD Negative of 1-Level Internal Channel

where the channel is split in two at each level was used. This specific geometry was chosen because previous iterations of parallel high-throughput devices with rows of parallel channels

connected to one inlet(Figure 3) were infeasible since the resolution allowed by these highly

viscous resins isn't sufficient for the width and height of the channel to be smaller than ~66um

and 30um respectively. By using this branched design, the flow is halved at every level to

evenly distribute the force and increase throughput to all final channels.

Additionally, by stacking the channels and splitting the flow using the same branched concept in a vertical manner for higher throughput (as shown in Figure 5), the number of
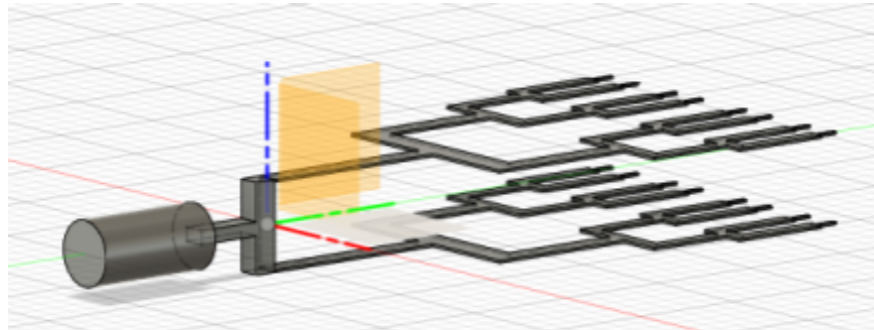

Figure 5: Stacked Branched Design

channels is doubled. This duplication process can be taken further by splitting the vertical

channel, which connects the two bifurcated designs. By introducing another division that

transforms one vertical channel into two, it's now possible to efficiently manage the flow division

and connect each to two channels. This design results in a total of four levels of bifurcation

instead of the two seen in Figure 5. Now, instead of the original eight outlets from a single

channel or 16 in Figure 5, 32 outlets from four channels can be achieved. Utilizing CAD

software, this process of mirroring or duplicating layers with minimal change becomes a

straightforward task, allowing for even greater throughput. This approach not only maximizes

the efficiency of the fluid flow within the device but also significantly expands the capacity of the

system, making it highly adaptable for various applications that require complex fluid

management on a compact scale.

In refining the initial branched microfluidic design created in Fusion 360, starting with the branched fork structure, solid material was extended from the end of the nozzle branches back to the beginning of the inlet. Next, the 'Combine' tool followed by the 'Cut' feature within Fusion 360 was used to subtract the fork structure from the newly added solid body, effectively removing the bifurcated fork along with the inlet. The outcome of this operation was a streamlined, solid
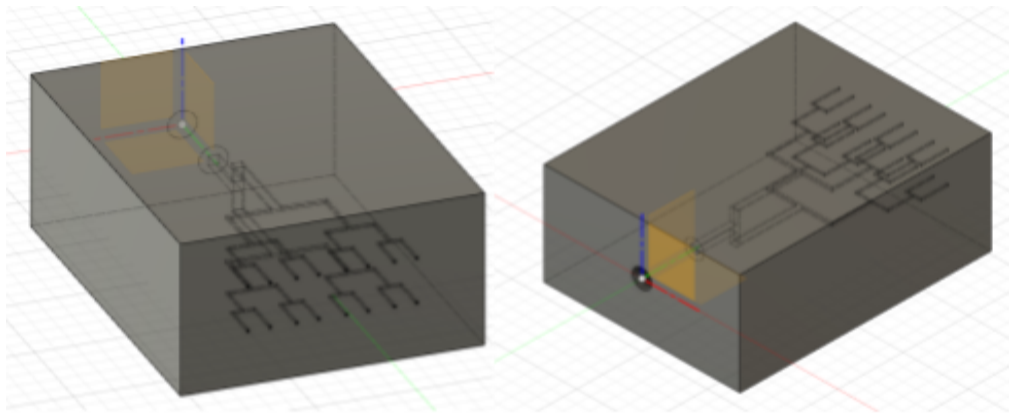

Figure 6: Front and Back of Bifurcated Device in Autodesk Fusion

microfluidic device that retained the channels for fluid flow but without the complexity of the external fork and inlet structures. This simplification refined the device's overall design and enhanced its manufacturability and structural integrity.

In the creation of our custom resin for 3D printing, a precise and tailored approach is adopted. The process begins with SirayaTech's Clear 'Blu' Resin, known for its mechanical strength, which forms the base of our resin mixture. The hydrophobic photoabsorber Sudan 1 is added at a concentration of 0.2%. This specific concentration was determined through extensive experimentation. Notably, as the concentration of Sudan 1 increases, the microfluidic channel resolution can be made smaller which would result in smaller microparticles. However, this reduction in channel size is a trade-off with the risk of failed prints due to non-adhesion of the prints at higher Sudan 1 concentrations, emphasizing the importance of maintaining the optimal range for successful 3D printing outcomes. It was observed that while a range of 0.05% to

0.25% of Sudan 1 is effective, exceeding the 0.25% threshold leads to significant issues, particularly concerning non-adhesion to the build plate and thus failed prints.

The actual printing involves the successive curing of the resin layer by layer to form the 3D structure of the microfluidic device. When the print is completed, the device is carefully detached from the build plate(Figure 7). It then undergoes a post-processing stage, which is crucial for removing any uncured resin. This involves washing the device and pumping ethanol through the internal structures. Ethanol effectively cleans out residual resin from the internal channels, ensuring that they are fully open and functional. The final step includes pumping ethanol through the entire device to test the fluid flow, verifying that most channels are indeed open. This step is crucial for confirming the practical usability of the microfluidic device since closed channels can create uneven pressure elsewhere in the device

Figure 7: Side-by-side comparison of printed microfluidic device and CAD drawing (l x w x h of 20x15x8mm) from Blu-Sudan 1 Resin

and cause other issues like rupturing. When these steps are completed satisfactorily the branched microfluidic device is now ready for use.

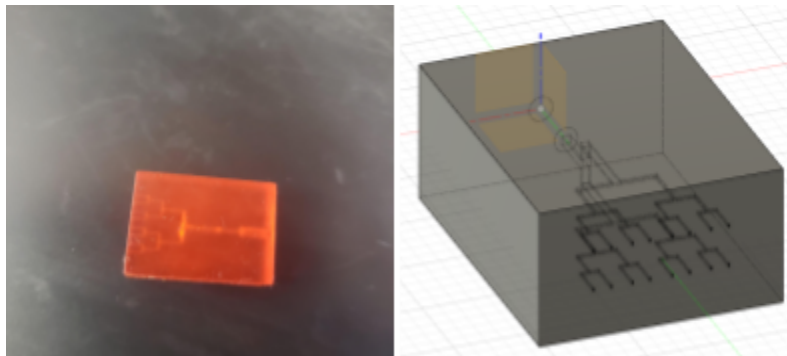3.4 Precursor composition of microparticles

The initial microparticles are mixed with one of three types of polyethylene glycol diacrylates (PEGDA) - 700, 575, or 250. The selection of the PEGDA variant is based on the desired properties of the final microparticles, such as porosity, mechanical strength, and degradation rate, which in turn would influence the drug release profile e.g. PEGDA 700 is known for having

higher porosity since the higher molecular weight leads to more space between cross-linked chains. The drug-PEGDA mixture is prepared under carefully controlled conditions to prevent any premature polymerization and to ensure that the drug molecules are evenly distributed throughout the polymer base. An important observation made during this phase is the impact of the drug concentration on the polymerization process. Higher concentrations of the molecules like fluorescein were found to hinder the effective polymerization of PEGDA. Therefore, in theory, maintaining an optimal, low drug concentration is essential to avoid negatively affecting the polymer matrix's integrity.

The final step in preparing the drug-loaded microparticles involves the addition of Irgacure 1173, a photoinitiator essential for triggering the polymerization process. Once the photoinitiator is incorporated, the mixture is exposed to controlled UV light at 365nm, initiating the crosslinking of Irgacure and the diacrylate(DA) ends the PEG for formation of the microparticles. After polymerization, these microparticles, now encapsulating the drugs, are analyzed for uniformity in size.

3.5 Microparticle fabrication

To create the microparticles requires a fairly simple setup. The process starts with a clear plastic cup-chosen for its transparency and compatibility with UV light- to stabilize the light source's placement. To generate the necessary UV exposure, a string of UV lights, specifically emitting at 365 nm, was
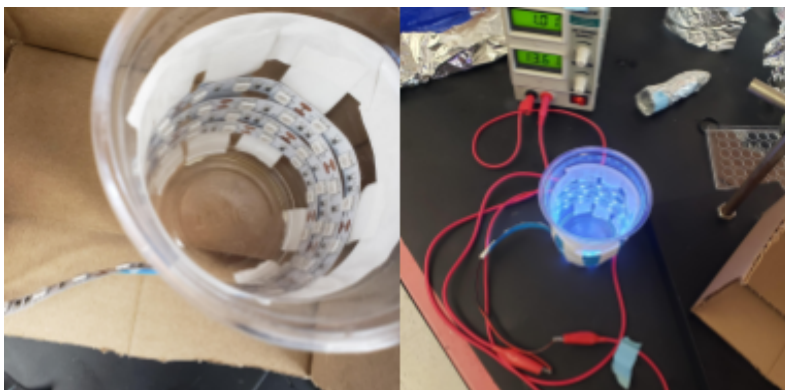

Figure 8: UV Lights(Left) attached to cup(Right)

carefully coiled and taped around the cup. This wavelength was selected for its effectiveness in initiating the crosslinking reaction of droplets dissolved with Irgacure 1173. To secure the lights in place and maintain an even distribution of UV exposure, regular tape was strategically applied over the coiled lights to help the strip stay fixed in the desired position around the cup. Notably, the ends of the UV light string were left exposed to allow an easy connection to a power supply. By connecting these ends to a suitable power source, the UV lights could be activated, providing a consistent and controlled source of UV light.

In the laboratory setup, we've adapted a clamp stand to hold a 50mL conical tube that will collect the final droplets. At the base of this clamp stand is positioned the previously described cup, now outfitted with a coil of UV lights.

Figure 9 - Setup using pump and UV Light to create microparticles

This setup allows us to place the conical tube directly above the UV light-emitting cup. By tightening the clamp, the tube is securely held in place, aligning perfectly with the UV source for optimal exposure.

Within this conical tube is the microfluidic device, attached to a syringe. This device is tasked with the critical role of managing the flow of our experimental mixture – the mixture comprising PEGDA, a solvent (either DMSO or water), the photoinitiator Irgacure 1173, and a fluorescent molecule. The 50mL tube is filled with a continuous-phase liquid, creating the ideal environment for droplet formation. The syringe, connected to a pump, applies a slow and steady pressure to push the fluid for the controlled and consistent formation of droplets. As the mixture is pushed

through the microfluidic device, it exits as individual droplets. These droplets, upon their descent into the conical tube, are immediately exposed to the UV light from the cup below. This exposure catalyzes the polymerization of the droplets, effectively 'freezing' them in their formed state into spherical microparticles.

Results:

4.1 Presentation of gathered data, including images, measurements, & other relevant results.

<u>Mineral Oil + Blue Dye Water running at 5000uL/min and 1000uL/min</u>

In initial experiments, the focus was on understanding the impact of flow rate on droplet size in a 3D-printed droplet generator submerged in mineral oil. Two different flow rates were tested using separate pumps: one at 5000 µL/min and the other at 1000 µL/min. The goal was to observe how varying the speed at which the water-blue dye fluid is pumped through the device would affect the characteristics of the droplets formed.
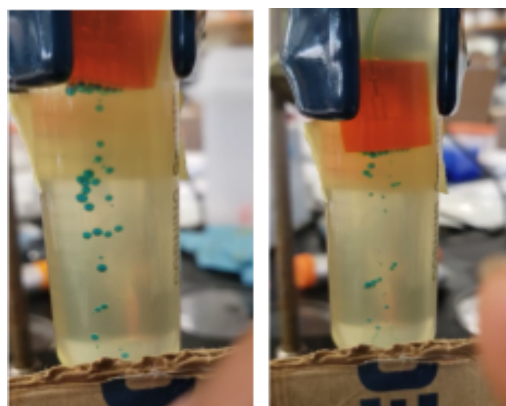

Figure 10a) Min. Oil at 5000uL/min

Figure 10b) Min. Oil at 1000uL/min

The first observation, evident in the video footage(Appendix) of the experiment, was that a higher flow rate resulted in the formation of larger droplets. At 5000 µL/min, it appeared that the increased volume of fluid arriving at the outlet led to an accumulation of more liquid before each droplet was pinched off. This observation aligns with fluid dynamics principles, where a higher flow rate typically provides a greater volume of fluid at the point of droplet formation, leading to larger droplets.

Furthermore, an interesting interaction was noted with the properties of mineral oil, the continuous phase in which the device was immersed. Mineral oil is known for its relatively high density(~0.86 g/mL) and viscosity – essentially, it's thicker than many other fluids. This increased thickness poses a greater resistance to the movement of the blue dye liquid used in the experiment. As a result, when the blue dye liquid is forced to move through the denser mineral oil at a higher flow rate, it encounters more resistance, contributing to the formation of larger droplets. This behavior underscores the significant role that the external medium – in this case, mineral oil – plays in the dynamics of droplet formation in microfluidic applications as heavy mediums such as mineral oil delay normal gravitational effects of pulling the droplet down, which in turn allows the droplet to stay at the channel's interface and grow in size until a critical mass is reached These findings provide valuable insights, particularly in the context of optimizing droplet-based systems for various applications, where control over droplet size is crucial.

Dodecane + Blue Dye Water running at 5000uL/min and 1000uL/min

In the second set of initial experiments, a lighter continuous-phase medium called dodecane was used to determine viscosity's effect on droplet size. Two separate trials involved a microfluidic device immersed in dodecane, to observe the effects of different flow rates on droplet formation. The experiments were again carried out with two distinct flow rates set for the pumps: one at 5000 μL/min and the other at 1000 μL/min.
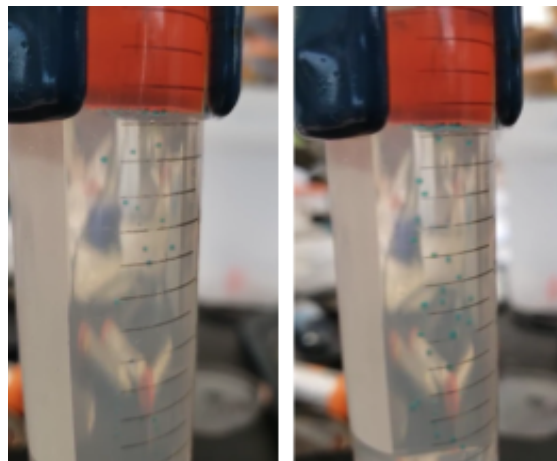

Figure 11a) Dodecane at 5000uL/min

Figure 11b) Dodecane at 1000uL/min

From the video analysis of the experiment(Appendix), it was immediately apparent that the flow rate plays a significant role in determining the size of the droplets. Specifically, the experiment running at a higher flow rate of 5000 µL/min resulted in the formation of notably larger droplets compared to the one at 1000 µL/min since these particles couldn't be solidified with UV light.

Another interesting observation was the influence of dodecane's properties on the droplet formation. Dodecane has a lower density(~0.75 g/mL) compared to many mineral oils (~0.86 g/mL), and this lighter density was reflected in the behavior of the droplets. In the video, the droplets in the dodecane not only
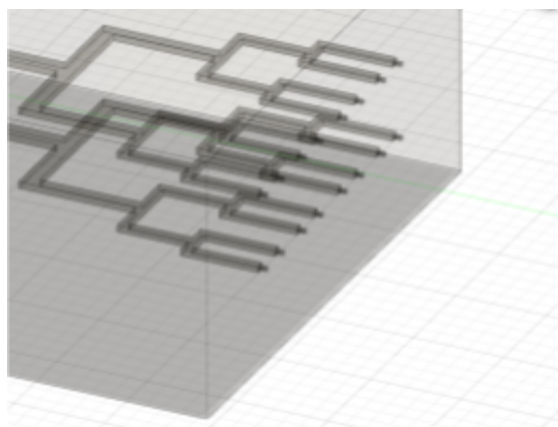

Figure 12: Device schematic with smaller dropgen outlets

appeared smaller but also fell much faster. This quicker descent and reduced size suggest that the lower resistance and lighter density of dodecane allow the droplets to detach more readily and move more swiftly once formed.

To optimize the microfluidic device design, a channel size of 220x200um was initially chosen, with the channel ends specifically reduced to 88x100um and extended to a length of 100um. This modification was implemented to stop device rupture, which occurred due to high pressures during the ethanol cleaning process when using uniformly small channels. To assess the impact of these design changes on droplet formation, blue water was run through the device, and the resulting droplets were characterized based on prior experience with similar setups. Interestingly, the droplets formed by this revised channel configuration appeared to closely match the size of those produced by the standard 220x200um channels, typically around ~700 um in diameter. By inspection, it was apparent that the blue liquid at the outlet

18

accumulates and expands until reaching a critical volume before detaching and falling into the surrounding dodecane as there was no shear force to minimize droplet size increase. This underscores the importance of shear forces in controlling droplet size, highlighting that shrinking channel dimensions don't seem sufficient to alter droplet sizes significantly without considering other factors involved in the droplet formation process.

Fluorescein Completely Inhibits Polymerization

In a series of experimental tests, polymerization of a mixture composed of a 1:3 ratio of PEGDA 700 and DI Water, with 2% Irgacure 1173 added as a photoinitiator was explored. For the trial, a 4mL solution was prepared and then equally divided into two separate vials. In one of these vials, the addition of even a minimal amount of fluorescein, as slight as 0.1%, had a dramatic effect - it completely inhibited droplet polymerization. The result was a transformation of the 2mL solution into a non-polymerized, gooey substance. This outcome starkly contrasted with the behavior of the solution in the second vial, where no fluorescein was added(Figure 13). This solution underwent successful and complete polymerization and created large droplet particles when cured by UV light.

Figure 13: MP Precursor w/(right) & w/o fluorescein(left)

From these contrasting results, it became evident that fluorescein sodium salt possesses properties that interfere with the polymerization process of this specific resin mixture. This interference was significantly more pronounced than with other fluorescent molecules that were tested, which also caused some issues with polymerization, but none to the extent of fluorescein(Figure 13). This discovery highlighted the need for careful selection of

fluorescent dyes in resin formulations, especially when considering their compatibility with the polymerization process in 3D printing applications.

In a new formulation, no fluorescent molecules were added. To create the microparticles, a mixture was prepared using PEGDA575 and DI water in a 1:1 ratio, totaling 4mL, with Irgacure 1173 added at a 5% concentration to initiate polymerization under UV light. The continuous phase consisted of dodecane enhanced with 3% Span 80 to stabilize the emulsion. This mixture was then processed through a microfluidic device with dimensions of 220x200 micrometers, employing a flow rate of 500µL/min, facilitated by a 3mL BD syringe. Upon exiting the device, the droplets were exposed to 365nm UV light, causing the PEGDA mixture to polymerize and form solid microparticles. The particles produced through this method ranged in size from 650µm to 1000µm, with the majority measuring approximately 700µm. The particles were
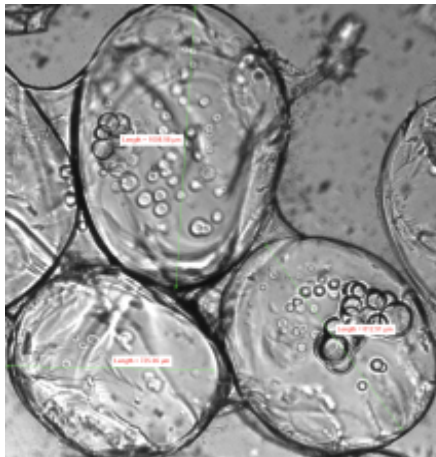

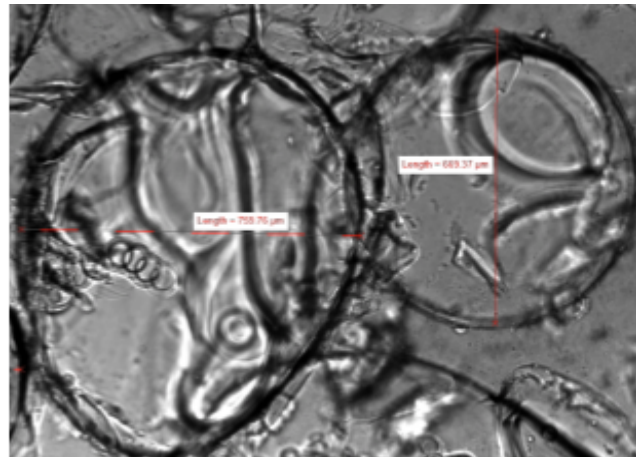Figure 14a: Particles captured on fluorescent microscope

Figure 14b: Particles captured on fluorescent microscope

unusually difficult to disaggregate which may have been due to higher concentration of PEGDA-575 at 1:1 with water vs a 1:3 ratio and 5% Irgacure 1173 since 2% is thought to be enough in most cases.

To accurately characterize the microparticles produced with the branched 220x200um channel and a dodecane solution with 5% Span 80, a fluorescent microscope (FScope) running the NIH Elements program was used. The FScope captured high-resolution images of the microparticles at a 4X magnification, providing detailed visual data. The images obtained have a scaling factor of 1.63 um/pixel, requiring an adjustment where each pixel measurement is multiplied by this factor to determine the true diameter of the microparticles.

For the analysis of the microparticle images, the program CellProfiler was utilized, specifically leveraging its 'ExportToSpreadsheet' module. This module generates many columns but specifically, one named 'AreaShape_EquivalentDiameter'(Table 1) that determined the average diameter of was 712um, with a standard deviation of 107um. This resulted in a coefficient of variation of approximately 0.15, indicating a relatively low degree of size variability among the microparticles. Such detailed analysis not only provides insight into microparticle uniformity but also underscores the utility of combining advanced imaging techniques with analytical software for detailed particle characterization.

NOVEC 7500 + Picosurf 2%

To address the issue of aggregation during UV crosslinking, NOVEC 7500 with 2% Picosurf was used as the continuous phase in a proof-of-concept experiment. This adjustment significantly
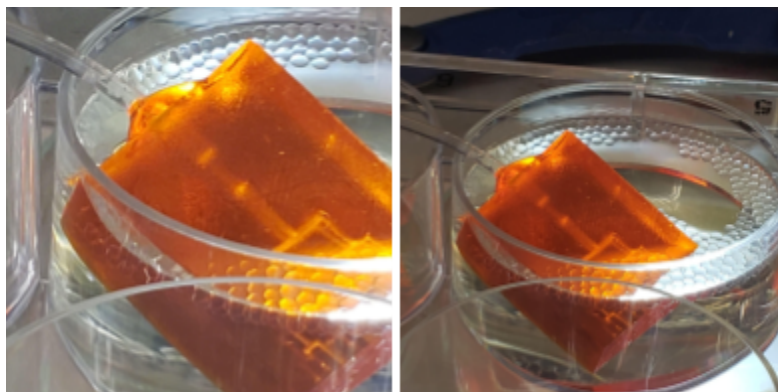

Figure 15: Particle production in NOVEC 7500 w/ 2% Picosurf

improved the droplet formation process, resulting in droplets that did not coalesce. The choice of the continuous phase proved to be a critical factor in achieving these stable droplets. It was observed that the channels closer to the surface produced droplets more efficiently, likely due to variations in pressure. With an optimized setup, throughput could be further improved. The device featured channels with dimensions of 220x200 µm, leading into a 500 µm x 88 µm x 60 µm 8-pronged, two-level channel configuration.

Small-Channeled Device Rupturing Upon Ethanol Cleaning

One of the primary challenges encountered in the process of 3D printing microfluidic devices has been cleaning them with ethanol without causing any damage. This issue becomes particularly problematic when attempting to reduce channel sizes that will reduce droplet size. While the printing process can successfully produce these smaller channels, the subsequent cleaning step with ethanol presents a significant hurdle. The high pressure required to push ethanol through tinier channels, due to the increased resistance from their reduced dimensions, often leads to the device rupturing and becoming unusable. This problem persists even when the design is modified so that only the final 10% of the channel has a smaller cross-section. This may be solved by using lower pressure, but the issue with this is high pressure is generally needed to fully release the maximum amount of channels and without it the throughput, i.e. the number of channels that can release, is low.

4.2 Implications of findings in the broader context of microfluidics and 3D printing

More Complex Designs Now Possible

The advancements demonstrated in the successful 3D printing of complex microfluidic devices hold significant implications for the broader field of microfluidics and its intersection with 3D printing technology. One of the most notable aspects of this achievement is the ability to rapidly iterate and test intricate designs. The capacity to print complex architectures and multi-level channels opens up new avenues in microfluidic design, particularly in creating maze-like channel structures. These elaborate channels can potentially be used to mix and separate fluids in more efficient and controlled ways, surpassing the capabilities of traditional, planar one-dimensional PDMS microfluidic devices.

Furthermore, the ability to print multi-level structures that can be bonded together paves the way for singular, integrated designs that were previously challenging or even impossible to fabricate using conventional methods. This capability can revolutionize the design and manufacturing of microfluidic devices, allowing for the creation of more compact, sophisticated systems. Such integrated multi-level devices could be especially beneficial in applications requiring complex fluid manipulations, such as in lab-on-a-chip systems where space is limited and functionality is critical.

Multiple Interconnected Prints

To maintain the simplicity of the shear-free device but control droplet size via a shear force, a two-outlet block with a void space was added. The first part retains the original design of the shear-free microfluidic device, featuring the stacked bifurcated channels that have proven effective in previous models. The second part of the device is specifically designed to

incorporate the void space necessary for the continuous phase liquid, along with appropriate inlets and outlets. By separating these two functional elements into different components, we can address the printing challenges associated with creating void spaces within a single, monolithic structure.
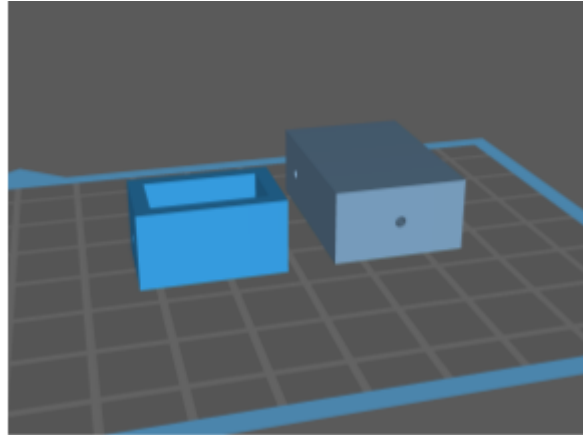

Figure 16: Multi-component design in Chitubox

The key to successfully printing the second part of the device, which includes the void space, lies in the orientation of the print. By strategically positioning the void component such that the side with the most material is printed first on the build plate, each successive layer of the print has a solid base to adhere to. This approach mitigates the problem of printing void spaces, as it allows for the necessary structural support throughout the fabrication process. By assembling these two parts post-printing, it's possible to create a composite device that encompasses both the efficient fluid handling of the shear-free design and the variable control over the continuous phase flowing in the void space. This two-part design(Figure 16) not only resolves the printing challenges but also opens up new possibilities in microfluidic device fabrication, allowing for more complex and functionally diverse chips.

Despite this approach, several downsides prevented droplet creation. Among these was the significant issue of leakage when the two components were assembled. Even after thoroughly cleaning the device and ensuring free flow through all channels, it consistently leaked when assembled. The process of connecting tubing for both the continuous and dispersed phases to the designated inlets didn't solve leakage, rendering the device incapable of producing droplets as intended. The elusive nature of the leaks, which were difficult to pinpoint to a single location and might have stemmed from multiple sources, further complicated troubleshooting efforts.

Although this setup did not work for the droplet generation, this modular design paradigm utilizing multiple interlocking components will almost certainly be useful in other areas.

Single Shear-Thinning Device: Good Idea, Bad Print

In an effort to create a shear-thinning microfluidic device, a design that innovatively incorporates the features of bifurcated channels similar to the shear-free devices previously developed, while also integrating a void
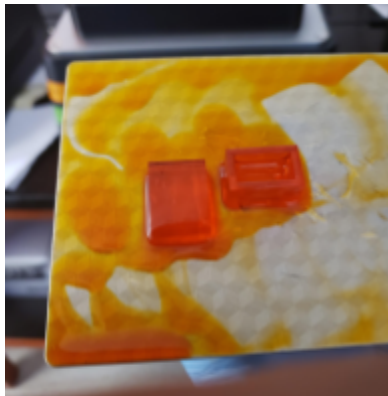

Fig. 17a) Multi-component device on build plate
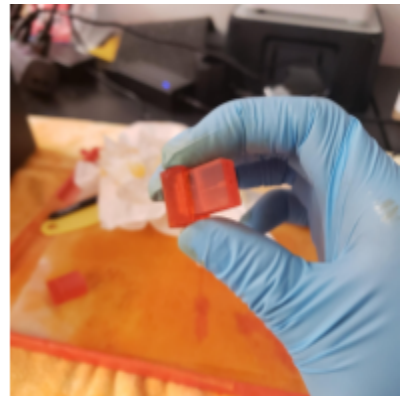

Figure 17b) Multi-component device interlocking

space for the continuous phase liquid to shear the droplets off. By implementing a programmable flow rate for the continuous phase, the device can apply variable shearing forces to the dispersed phase. This ability to modulate the shear force dynamically is expected to provide more direct control over the size of the droplets produced. The concept hinges on the principle that different shear rates can influence the breakup of the dispersed phase, thereby enabling precise manipulation of droplet size.

However, this design presents a unique challenge since the inherent limitation of 3D printing technology is that each successive layer of material needs to adhere to the layer beneath it, with the exception of the first layer, which adheres directly to the build plate. Therefore, creating an empty space within the device – essential
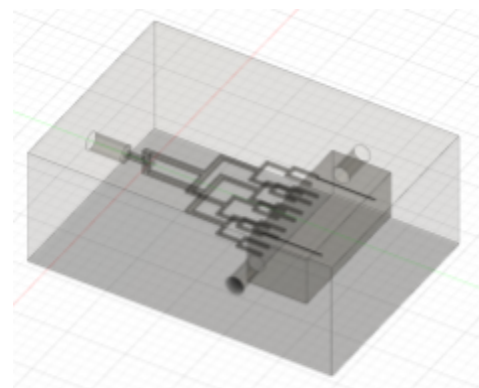

Figure 18: Shear-thinning device w/ oversized continuous phase cavity

for its intended function – disrupts this layer-by-layer building process as the void space lacks a solid base for the subsequent layers to adhere to, leading to potential structural integrity problems in the printed device, if it even prints at all. When running this test, surprisingly the device successfully printed!
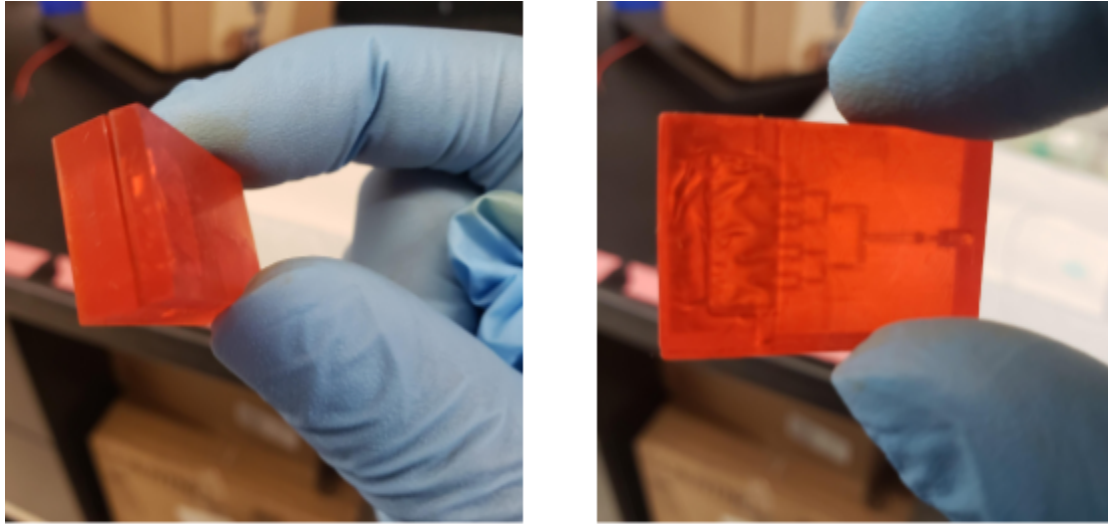

Figure 19. Destabilized print from oversized continuous phase cavity

However, it was observed that the printed structures were fairly fragile, particularly at the layers where the internal void space was located. This inherent weakness led to frequent breakages at these critical points, posing significant challenges to the device's structural integrity. In the devices that maintained their integrity, cleaning the internal void proved to be difficult, as seen by the orange resin discovered within the void space when the device broke apart. Despite multip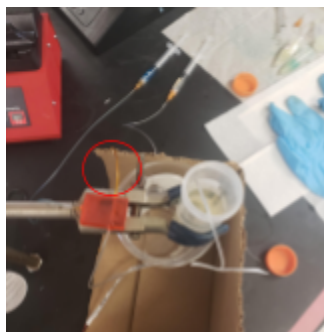le attempts at cl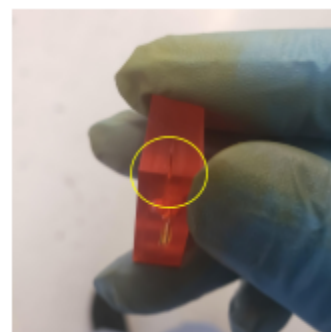eaning with ethanol, the resin's presence highlighted the difficulties in maintaining a clean continuous phase space to shear the droplets.

Figure 20a) Trapped resin(red circle)

Figure 20b) Destabilized prints after initial use

It can also be seen from Figure(20a) that excess orange resin was backing up into the continuous phase syringe, but not the outlet tubing that leads into the conical tube. Further runs showed the same problem where even though the device did not rupture immediately, it did break down along the same layers(Figure 20b) after tubing was solidified in place using Norland Optical Adhesive 81(NOA 81) under 365nm and the dispersed phase and continuous phase were pumped at 100uL/min and 160uL/min respectively. These were not abnormally high pressures as the shear-free branched design could handle single inlet pressures of up to 5000uL/min.

Single Shear-Thinning Device Improvements

In refining the shear-thinning device, a significant improvement was achieved by reducing the width of the internal void space from 5mm to 1.5mm. This modification not only enhanced the structural stability of the device, preventing it from breaking down during initial 3D print and use, but also yielded better functional results. Using a mixture

Figure 21 Shear-thinning device w/ smaller continuous phase cavity

of water with blue dye as the dispersed phase and dodecane with 2% Span 80 as the continuous phase, the device successfully produced smaller droplets, as observed through visual inspection.
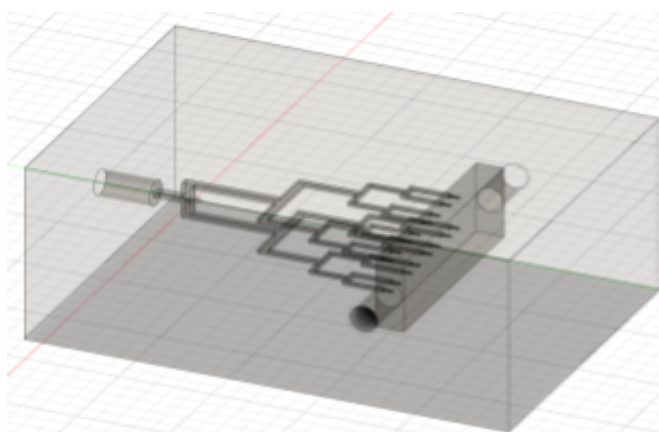
Adjusting the design of the single microfluidic device to reduce the continuous phase void space from 5mm to 1.5mm resulted in a significant improvement in the device's structural integrity. This modification allowed for successful droplet production, although the initial attempts revealed issues with crosslinking efficiency, likely due to insufficient polymer concentration and short exposure time. It
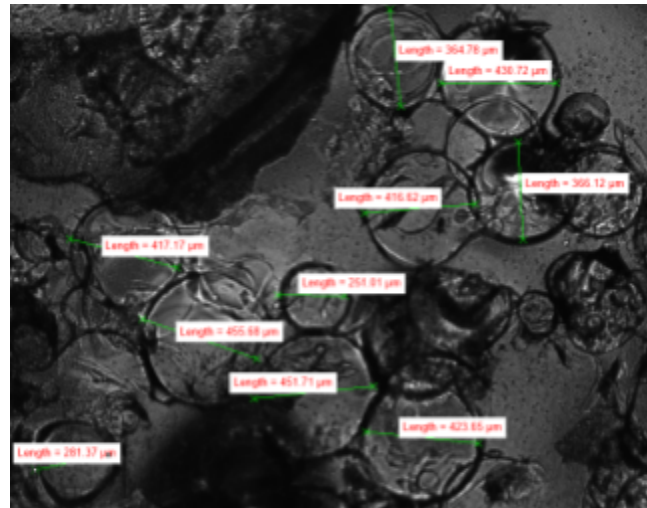

Figure 22a) Aggregated droplets profiled by CellProfiler

was apparent that droplets were being produced but were clumped into a solid mass as other

previous iterations, like this attempt, used dodecane + Span 80 for the continuous phase. In an attempt to address one part of this, the concentration of the polymer solution was increased, shifting from a 3:1 ratio of DI Water and PEGDA 575 to a more concentrated 1:1 ratio. This adjustment in polymer concentration with
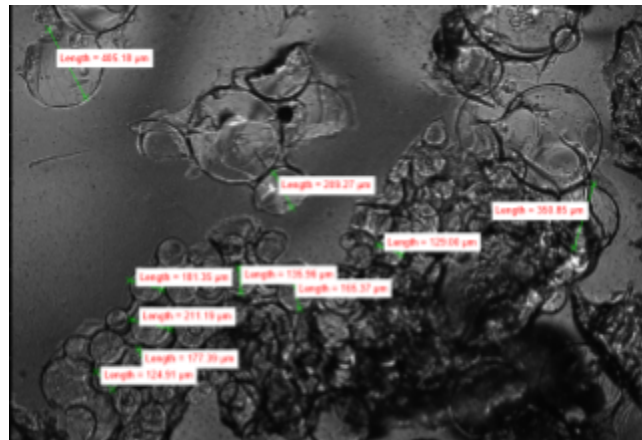
Figure 22b) Aggregated droplets in CellProfiler

the device running at 50uL/min(dispersed flow rate) and 200uL/min(continuous phase) led to the formation of droplets with bimodal average diameters between 100 um and 500 um, indicating a wider range of droplet sizes being produced from channel size length, width, and height of 500x88x150um. The increase in polymer concentration also caused droplets to clump together, posing potential obstacles to uniform droplet formation and subsequent applications of the microparticles. This will likely be solved by using UV light to crosslink particles for >1 minute

when particles are not going to be in contact with each other and removing the UV source when they are collected so they do not continue to crosslink.
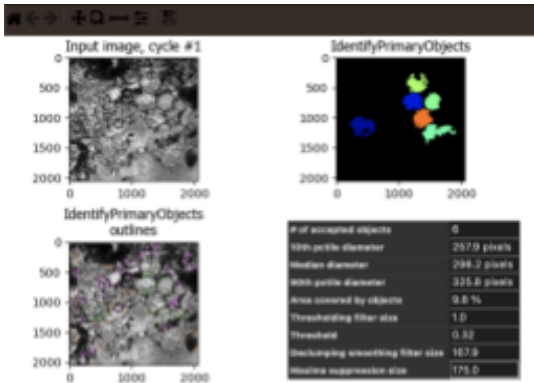

Figure 23 CellProfiler example of droplet characterization

The clumping of droplets posed significant challenges in characterizing the microparticles using CellProfiler, a software designed for analyzing cell images. When particles adhere to each other, the software struggles to separate and accurately identify the edges of individual droplets, complicating the analysis process. This difficulty was evident in the recent batch of images, where many captured droplets appeared non-circular and irregular in shape, deviating from the expected profiles. To mitigate this issue, attempts were made to filter out these irregularly shaped particles using CellProfiler's settings. However, this approach introduced a degree of non-randomness to the selection process, potentially skewing the data. From the analysis, as seen in Figure F2 at 4x magnification with a pixel/um ratio of 1.63, the median diameter was calculated to be around 300 pixels, equivalent to 492um.

Branched Parallel Stacked Design

A final design inspired by the original 200-channel parallel droplet system(de Rutte 2019) was tested. This design featured two layers of droplet generators connected to a continuous phase shear outlet profile with a compressed 2D shape. The precursors used for this test were PEG575 and water at a 1:3 ratio, with 3% Irgacure 1173. These droplets were not polymerized but were characterized under the fluorescent microscope (FScope).
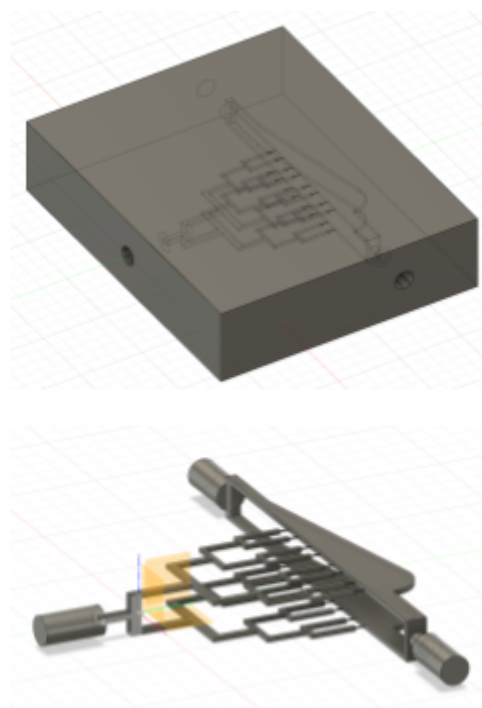
Figure 24 Microfluidic device with compressed cavity for improved droplet shearing

Two flow rates were tested to observe the droplet size distribution. At the first flow rate of 25 µL/min for the dispersed phase and 100 µL/min for the continuous phase, the droplets exhibited a bimodal distribution. The larger droplets had an average diameter of 768.92 µm, while the smaller droplets averaged 213.76 µm. At the second flow rate of 10 µL/min for the dispersed phase and 100 µL/min for the continuous phase, the

Figure 25 a) 25x100 uL/min dispersed & cont. phase & respectively

b) 10x100 uL/min dispersed & cont. phase & respectively

bimodal distribution persisted. The larger droplets again averaged 503.67 µm, but the smaller

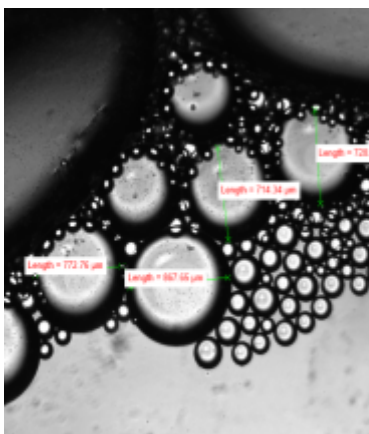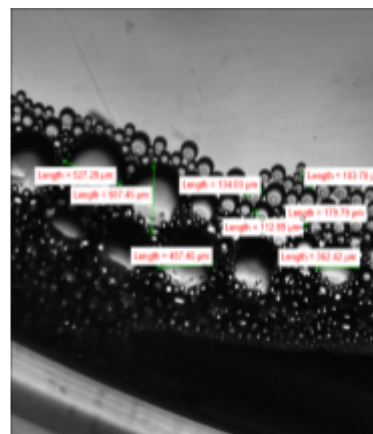droplets averaged 145.685 μm. Droplets seem to crowd the edges of the well plate so while

many were captured, many others were obfuscated by less light near the rim.

Discussion:

5.1 Interpretation of results

The presence of fluorescein in the setup hindered the formation of microparticles, as evidenced

by the droplets consistently solidifying into a mass at the bottom of the conical tube. In contrast,

when there was no fluorescein and there was an even PEGDA to water ratio, the creation of

droplets was generally successful. This discrepancy suggests that fluorescein may be

interfering with the polymerization process, potentially by absorbing the UV light necessary for

activating the crosslinking reaction between Irgacure 1173 and PEGDA 575. Given this, it's

advisable to employ dye-mixed water or water with no dye at all when visually monitoring

droplet formation before moving to cross-linkable polymers. Adding fluorescent molecules

during the actual microparticle production process should be avoided, as the successful

polymerization of the particles can be confirmed post-process with computer-aided

microscopes, eliminating the need for dyes that might compromise the reaction.

5.2 Challenges faced and potential solutions

During the experiment, droplets were successfully produced using a 1:3 mixture ratio of PEGDA

575 to DI Water with 5% Irgacure 1173, but a significant challenge arose when these droplets

coalesced at the bottom of the collection area and underwent hardening upon exposure to

365nm UV light. To mitigate this issue, the PEGDA 575 concentration was adjusted to a 1:1

ratio with DI Water, which improved the situation to some extent by preventing the droplets from

coalescing as heavily, though they still tended to clump together. This clumping posed a

problem for characterizing the droplets under magnification, necessitating a manual process of

applying pressure to break them apart for analysis.

A potential solution to overcome these challenges could involve redesigning the experimental

setup to allow for a more controlled crosslinking process. By implementing a system where

droplets can be crosslinked under UV light for a precise duration, possibly tens of seconds,

before being automatically transferred to a light-free collection reservoir, it might be possible to

prevent droplets from coalescing or hardening prematurely into the problematic clumps. This

approach would not only facilitate the production of more distinct and separate droplets but also

simplify the process of characterizing them post-production, eliminating the need for manual

intervention to break apart clumped droplets.

Conclusion:

6.1 Summary of the main findings

This study demonstrated methods for manufacturing scalable microfluidic devices utilizing

commercially available 3D printers and free CAD and slicer software. The experiment involved

leveraging the capabilities of 3D printing to fabricate multi-level internal microfluidic structures

that are often challenging to produce using traditional methods such as with PDMS gel.

Throughout the project, various design iterations were tested, including modifications to channel

dimensions and the integration of features like bifurcated channels and continuous phase void

spaces. Using a stacked bifurcation device with a smaller, flatter cavity, the design increased

pressure and more effectively sheared droplets. Testing at a 4-to-1 continuous phase to

dispersed phase ratio, and subsequently at a 10-to-1 ratio, resulted in a noticeable reduction in

droplet size of approximately 30%. Achieving sub-200µm droplets, specifically the ~145um

microparticle size, is particularly promising for extended drug delivery applications, as particles

typically need to be less than 200µm for needle injection.

However, several challenges remain. It is difficult to troubleshoot flow issues inside the device

due to its translucency, making it hard to properly profile throughput. Additionally, there is a need

to further shrink the device channels, increase throughput, and avoid producing bimodal particle

sizes, though the bigger particles can likely be filtered out. Despite these challenges, the

findings underscore the potential of 3D printing as a versatile and cost-effective tool for creating

complex microfluidic devices.

6.2 Potential applications of research

The research conducted on microfluidic devices has shown a promising avenue for potential

applications. One significant insight is the enhanced control over droplet size afforded by the

integration of a continuous phase void space within the device. By fine-tuning flow rates, there's

a tangible pathway toward achieving much smaller particle sizes, potentially reaching sub-100

um or even sub-50 um dimensions. It can be further amplified with advancements in 3D printing

technology where the smallest pixel width is less than 22um, which is the current affordable

printer resolution. This would allow even more precise channel dimensions, opening up new

possibilities in fields requiring fine particulate control, such as particles for medical applications

and precision manufacturing.

The introduction of a branched design within the microfluidic device presents another exciting prospect. This design facilitates the creation of even-pressure systems across a wider array of channels, significantly enhancing throughput without compromising performance. While adding more branches in CAD software can be a bit more complex, the design inherently allows for growth in the number of channels by a factor of 2^n. This feature is particularly promising for applications requiring high throughput in a compact space.

Lastly, the research paves the way for the development of multi-level, maze-like microfluidic designs that overcome traditional 2D constraints, allowing channels to be created in all three dimensions. This advancement could drastically improve the design of lab-on-a-chip devices, offering greater complexity and functionality. Such devices could find applications in diagnostic tests, chemical reactors, or biological studies, where the mixing of multiple fluids and reactions in a three-dimensional space can be fully harnessed.

6.3 Recommendations for future research

One of the critical challenges in device fabrication is finding an effective method to clean them without causing ruptures and breakages. A potential solution is to modify the device design, specifically by enlarging the channel dimensions. Increasing the channel size would allow fluids to pass through at lower pressures, thereby reducing the risk of device damage during the cleaning process. However, to maintain the desired functionality, such as precise droplet formation, the outlet dimensions could be kept small for the last 10% or so of the channel. This adjustment requires a careful balance between ease of cleaning and device performance, highlighting the importance of iterative design in optimizing microfluidic devices.

Additionally, the scalability of these devices for industrial applications remains an area for further investigation. The current designs may not offer the high throughput necessary for industrial-scale production, suggesting that further improvements may be required especially on larger printers with a greater vat and build plate area. Identifying larger production machines and internal design modifications that can enhance throughput without compromising the device's functionality or integrity is important for moving microfluidic technologies from the laboratory to industrial settings.

Applying silane to coat the surfaces of microfluidic devices is an additional approach to enhance their droplet creation by making the surfaces more hydrophobic. However, the process of silanization is not without its challenges. The treatment requires a significant drying time to ensure the silane has properly adhered to and modified the surface, which can slow down the overall device fabrication process. Additionally, ensuring the success of the silanization can be difficult since the device channels are completely enclosed, making it challenging to directly determine whether the treatment has uniformly covered all necessary surfaces and achieved the desired hydrophobic effect.

On another front, the use of NOVEC 7500 in tandem with Picosurf has shown promise in stabilizing droplet formation within microfluidic devices by allowing droplets to rise and pinch off more rapidly, likely due to the lighter molecular weight of NOVEC 7500 as the continuous phase. However, the manufacturer-led phase-out of NOVEC by the end of 2025 creates issues in the long-term viability of research based on this substance. It may be worthwhile to shift the focus towards optimizing other aspects of the microfluidic process that do not depend on materials with uncertain futures or prohibitive costs, ensuring the research remains relevant and sustainable in the long term.

Hydrophilic resins, combined with suitable photoabsorbers like tartrazine, present an avenue for creating devices that can produce hydrophobic particles. The current challenge lies in overcoming the wetting issues associated with using hydrophilic materials in the fabrication process. The development and implementation of hydrophilic resins in microfluidic device production could significantly advance the field, enabling the use of a wider range of hydrophobic reagents. This would not only expand the capabilities of microfluidic devices but also open up new possibilities to create hydrophobic microparticles that can store hydrophobic drugs to treat disease, especially ones that are needed to pass the blood-brain barrier. This would be a boon to the combinatorial drug space since drug delivery is limited in delivering drugs of hydrophilicity and hydrophobicity.

In conclusion, this study contributes valuable insights into the development of microfluidic devices via 3D printing, presenting a pathway to more accessible and adaptable microfluidic technologies without the need for an expensive cleanroom that many labs simply will not have access to. Future work in this area could further refine the printing processes and materials used, potentially opening up new avenues for research and application in fields ranging from biomedical engineering to chemical analysis. The ability to rapidly prototype and test microfluidic designs through 3D printing not only accelerates the development cycle but also encourages innovation in the design of microfluidic systems.

Conflict of Interest

The author declares no conflict of interest.

BIBLIOGRAPHY

de Rutte J., Koh J., Di Carlo D. (2019). Scalable High-Throughput Production of Modular Microgels for In Situ Assembly of Microporous Tissue Scaffolds. Advanced Functional Materials. https://doi.org/10.1002/adfm.201900071

Walsh, D. I., 3rd, Kong, D. S., Murthy, S. K., & Carr, P. A. (2017). Enabling Microfluidics: from Clean Rooms to Makerspaces. Trends in biotechnology, 35(5), 383–392. https://doi.org/10.1016/j.tibtech.2017.01.001

Jayamohan, H., Sant, H. J., & Gale, B. K. (2013). Applications of microfluidics for molecular diagnostics. Methods in molecular biology (Clifton, N.J.), 949, 305–334. https://doi.org/10.1007/978-1-62703-134-9_20

Damiati, S., Kompella, U. B., Damiati, S. A., & Kodzius, R. (2018). Microfluidic Devices for Drug Delivery Systems and Drug Screening. Genes, 9(2), 103. https://doi.org/10.3390/genes9020103

Xiangdong Xue, Mayur K. Patel, Maïwenn Kersaudy-Kerhoas, Marc P.Y. Desmulliez, Chris Bailey, David Topham (2011) Analysis of fluid separation in microfluidic T-channels. Applied Mathematical Modelling. Volume 36, Issue 2, February 2012, Pages 743-755. https://doi.org/10.1016/j.apm.2011.07.009

Scott, S. M., & Ali, Z. (2021). Fabrication Methods for Microfluidic Devices: An Overview. Micromachines, 12(3), 319. https://doi.org/10.3390/mi12030319

Lin, L., & Chung, C. K. (2021). PDMS Microfabrication and Design for Microfluidics and Sustainable Energy Application: Review. Micromachines, 12(11), 1350. https://doi.org/10.3390/mi12111350

Tatiana Trantidou, Anna Regoutz, Xian N. Voon, David J. Payne, Oscar Ces. A "cleanroom-free" and scalable manufacturing technology for the microfluidic generation of lipid-stabilized droplets and cell-sized multisomes. Sensors and Actuators B: Chemical, Volume 267, 2018, Pages 34-41, ISSN 0925-4005, https://doi.org/10.1016/j.snb.2018.03.165